Nuclear Instruments and Methods in Physics Research B 267 (2009) 1317–1320

Contents lists available at ScienceDirect

Nuclear Instruments and Methods in Physics Research B

journal homepage: www.elsevier.com/locate/nimb

Impact of Ni co-implantation on Si nanocrystals formation and luminescence

J.F. Desjardins [a], M. Chicoine [a], F. Schiettekatte [a,*], D. Barba [b], F. Martin [b], G.G. Ross [b]

[a] Regroupement Québécois sur les Matériaux de pointe, Département de Physique, Université de Montréal, Montréal, Québec, Canada H3C 3J7
[b] INRS-Énergie, Matériaux et Télécommunications, Varennes, Québec, Canada J3X 1S2

ARTICLE INFO

Article history:
Available online 6 February 2009

PACS:
81.07.Bc
78.67.Bf

Keywords:
Silicon nanocrystals
Luminescence
Nickel
Ion implantation
Co-implantation
Nucleation
Time-resolved luminescence

ABSTRACT

We investigate the Si nanocrystals (Si-nc) growth and photoluminescence (PL) obtained by Si and Ni co-implantation. After 1 h of annealing at 1000 °C, PL emission between 600 and 1000 nm is observed to be five times higher for samples containing 0.04–0.21 at.% Ni than for samples without Ni. For samples annealed at 1100 °C, a small increase in PL intensity is observed followed by a decrease for Ni contents above 0.3 at.%. Our results are well described by a simple model which assumes that Ni atoms act both as a nucleation center for amorphous Si (a-Si) clusters crystallisation and as a non-radiative recombination site when more than one atom is included in a Si-nc. The nucleation effect is supported by the increase in PL intensity, the increase of PL decay time and the decrease of the a-Si Raman peak intensity at 480 cm^{-1} for samples annealed at 1000 °C in presence of ~0.1 at.% Ni. Time-resolved PL shows that Ni mainly affects two emission bands. The first band, around 730 nm, is related to an oxygen surface state, suggesting that Ni enhances oxygen bonding with Si-nc. The second band, around 880 nm, is associated to the crystallisation effect induced by Ni at lower annealing temperature.

1. Introduction

Since the first report of significant photoluminescence (PL) from porous silicon [1], extensive research has been undertaken to understand theoretically and experimentally the physics behind this effect in order to reach the feasibility of Si-based optoelectronic devices. It has been shown for example that Si nanocrystals (Si-nc) produced by ion implantation or chemical vapour deposition are also good light-emitters [2–4]. However, the emitted intensity needs to be increased in order to be useful for applications. Ways of improvement include better emission efficiency and an increase in Si-nc concentration. It is well established that Ni significantly decreases the Si crystallisation temperature through the formation of $NiSi_2$ [5]. Recent studies [6,7] have shown that the introduction of a Ni interlayer enhances the phase separation, leading to a larger number of smaller Si-nc and an increase in luminescence from Si-rich silicon oxide films (SRSO).

In this paper, we investigate the effect of Ni co-implantation on the formation and PL intensity of Si-nc obtained by ion implantation. It is shown that while small concentrations of Ni improve the nucleation process, larger amounts are detrimental to the emission efficiency.

2. Experimental details

Si nanocrystals were synthesised in amorphous fused silica samples that were co-implanted with 33 keV Si^- ions followed by 57 keV Ni^- ions. Energies were selected so that their mean projected ranges (R_P) are similar. Si ions were implanted at fluences ranging from 2.05×10^{16} to 5.7×10^{16} Si^-/cm^2, which correspond to peak Si excess concentration (Si_{xs}) at R_P of 6–15 at.%. Ni^- ions were implanted at fluences ranging from 2.9×10^{13} to 1.3×10^{15} Ni^-/cm^2, representing a local Ni concentration of 0.01–3 at.% at R_P. To activate the nucleation of Si-nc, implanted samples were annealed at temperatures between 950 and 1100 °C during 1 h under a nitrogen atmosphere. Samples were then passivated by a 5% H_2, 95% N_2 forming gas annealing at 500 °C during 30 min, in order to reduce the non-radiative recombination centers (NRRC) such as dangling bonds [8–10].

PL spectroscopy was carried out by using the 488 nm line of a 30 mW Ar-ion laser focussed on a spot of 1 mm in diameter. All PL spectra were measured at room temperature using an Oriel spectrometer and a silicon detector. The data were corrected to take the instrumental spectral response into account. Time-resolved PL spectra (TRPL) were measured at room temperature using a 405 nm diode laser powered at 50 mW on a 2 mm diameter spot. The pump time was set to 300 μs, with a transition time of 5 ns. Detection was carried out using a Ag–O–Cs photomultiplier (Hamamatsu R5108). Si-nc were characterized with a JEOL JEM-2100 transmission electronic microscope (TEM).

* Corresponding author.
E-mail address: francois.schiettekatte@umontreal.ca (F. Schiettekatte).

0168-583X/$ - see front matter © 2009 Published by Elsevier B.V.
doi:10.1016/j.nimb.2009.01.145

3. Results and discussion

Fig. 1 presents the PL spectra from 9 at.% Si_{xs} samples with different Ni concentrations annealed at 1000 °C. The PL spectra extend between 650 and 950 nm, peaking around 780 nm, although the position of the maximum changes with the Ni concentration. This annealing temperature is fairly low compared to the optimal annealing temperature of 1100 °C without co-implanted Ni [11]. Actually, the PL intensity is relatively low for samples without Ni, but increases dramatically with the addition of small amounts of Ni up to a concentration of 0.15 at.%. At this concentration, the peak intensity is five times higher than that of the sample without Ni. Ni concentrations greater than 0.2 at.% lead to a decrease of the PL intensity.

However, for all Ni contents, the PL intensity remains lower than for samples annealed at 1100 °C. This is shown in Fig. 2, where the integrated PL intensity of samples prepared simultaneously but annealed at 1000 and 1100 °C is plotted as a function of the Ni content. It is seen that after an annealing at 1100 °C, the PL intensity increases slightly but then decreases for greater Ni concentration. This is in contrast with the observations in SRSO [6,7] where PL intensity is reported to increase by a factor of 3 for Ni concentrations of ~1 at.%.

TRPL over the entire emission spectrum was measured in order to better understand the recombination dynamics. The PL intensity decay is not exponential and its shape varies with the Ni contents, changing from a stretched exponential to a power law at higher Ni concentrations (not shown). Since no single set of parameters can be used to characterize the decays, we extracted from each curve $\tau_{1/e}$, the time needed for the intensity to decrease by a factor $1/e$ from its initial value. By doing so, only the processes occurring on a time scale of the order of 10–100 μs are revealed. In Fig. 3(a) we report the $\tau_{1/e}$ values as a function of the emission wavelength extracted form TRPL measurements on samples annealed at 1100 °C. First, we notice that in absence of Ni, $\tau_{1/e}$ increases linearly with the emission wavelength up to about 880 nm. The linear shape suggests the presence of one major radiative recombination mechanism in which the quantum confinement model (QCM) plays a dominant role. Since larger wavelengths are generally associated to larger Si-nc by the QCM [12], the radiative recombination decay time increases with Si-nc size. According to [12], the decay time depends exponentially on emission energy, but over our restricted wavelength range, the dependence is fairly linear. Larger Si-nc contributes significantly to the emission at wavelengths greater than 880 nm. The number of structural defects increases with Si-nc size, enhancing the contribution of non-radiative transitions thus decreasing $\tau_{1/e}$ at greater wavelengths. Emission at these wavelengths can also come from smaller Si-nc containing interface defects or impurities, which in-

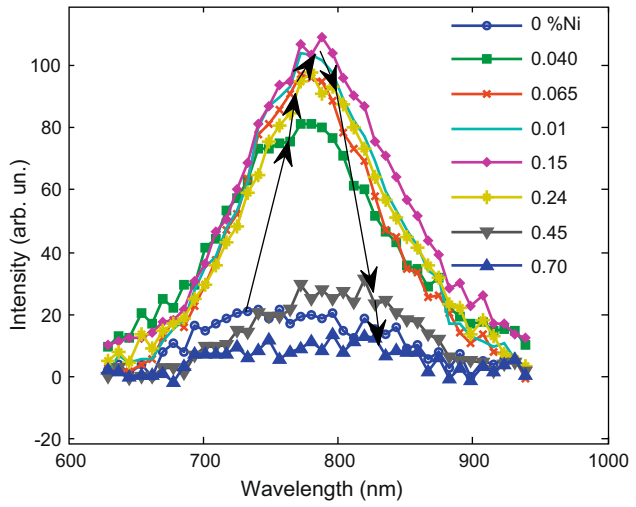

Fig. 1. PL spectra from samples containing 9 at.% Si_{xs} and annealed at 1000 °C for 1 h with corresponding atomic Ni concentrations.

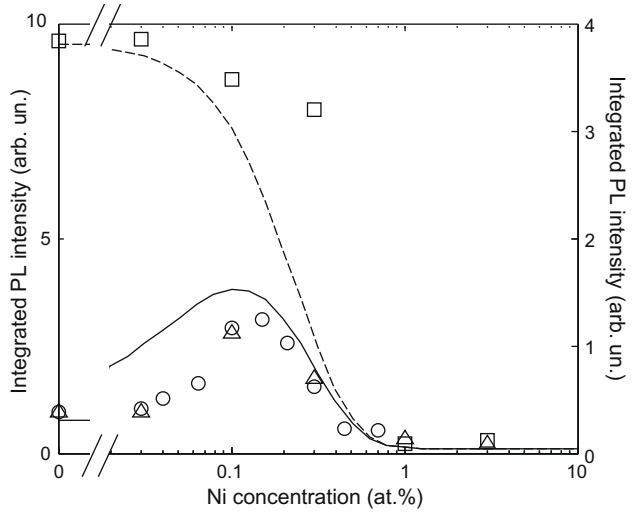

Fig. 2. Symbols: integrated PL intensity as a function of Ni concentration for a series of samples containing 9 at.% Si_{xs} and annealed at 1000 °C (triangles) and 1100 °C (squares) prepared and measured in nominally identical conditions. Circles, plotted against right axis, represent the integrated spectra of Fig. 1, and measured in different conditions. Curves: model considering a fraction of already crystalline Si clusters $p = 7\%$ (solid) and $p = 100\%$ (dashed).

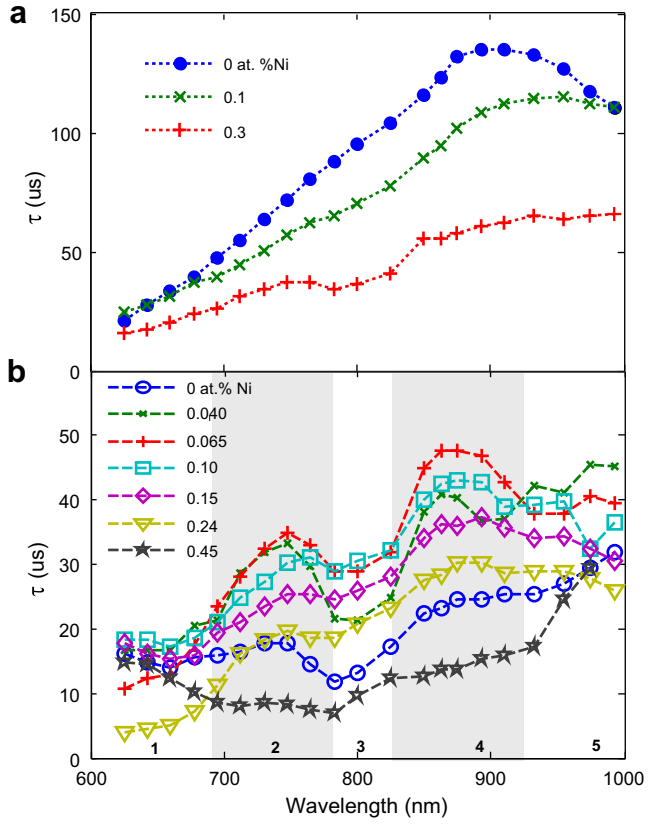

Fig. 3. Value of $\tau_{1/e}$ as a function of wavelength, for indicated at.% Ni concentrations. Samples have been annealed at 1100 °C (a) and 1000 °C (b). Numbers 1–5 in (b) designate the bands discussed in the text.

duce shorter decay times. We also observe in the same figure that $\tau_{1/e}$ decreases in presence of increasing amounts of Ni. This suggests that Ni acts mainly as a NRRC. The decrease in PL intensity is thus the result of an increasingly larger number of excitons recombining on non-radiative Ni-related centers, whose role is discussed below.

Looking now at TRPL measurements for samples annealed at 1000 °C presented in Fig. 3(b), it is seen that $\tau_{1/e}$ values are smaller than for samples annealed at 1100 °C, but show characteristic bands with larger decay times. It is also seen that $\tau_{1/e}$ first increases with Ni contents, and decreases at greater Ni concentrations, as observed for the PL intensity. The $\tau_{1/e}$ spectral dependence was divided into five emission bands, represented in Fig. 3(b). Data analysis reveals that bands 1 and 5 have a similar behaviour since $\tau_{1/e}$ increases with 0.03 at.% Ni and then decreases with higher concentrations. For band 3, $\tau_{1/e}$ increases with Ni concentrations of up to 0.1 at.% and then decreases. For bands 1, 3 and 5, $\tau_{1/e}$ is fairly linearly dependent on wavelength, suggesting that the emission within these bands originates from the quantum confinement mechanism. Bands 2 and 4 also have a similar behaviour since $\tau_{1/e}$ increases for Ni concentrations of up to 0.065 at.% and then decreases. However, these zones feature longer decay times. This behaviour suggests that new recombination channels with longer lifetime and higher capture cross-sections are available for the emission. Kanemitsu et al. [13] report that oxygen-passivated Si-nc emit around 730 nm from surface state recombination processes. This emission wavelength corresponds to the center of band 2 and suggests that Ni induces a modification of the atomic structure of Si-nc by favouring the formation of Si-O bonds at their surface.

Band 4 cannot be a result of Ni inclusion itself on the electronic structure since no similar band is present in Fig. 3(a). However, the introduction of Ni clearly has an influence on the time constant in this band, indicating that Ni can create or eliminate radiative transitions within this band. Raman scattering measurements (not shown) indicate a decrease of the phonon peak at 480 cm^{-1} (associated with amorphous Si TO-like line) and an increase of the 520 cm^{-1} peak (related to the Si-Si bonds in crystalline Si) with increasing amounts of Ni. This result shows that Ni promotes crystallisation of amorphous Si (a-Si). Hence, Ni enhances a-Si crystallisation, as observed for bulk a-Si [5], and tends to eliminate structural or bond defects within Si-nc or at the SiO_2/Si-nc interface. Defects removal eliminates at the same time some NRRC and leads to an increase of $\tau_{1/e}$ within this band.

However, it is known that Ni in c-Si adds a donor level above the valence band and an acceptor level under the conduction band [14,15]. Such a level can trap the charge carriers, creating new recombination channels with a redshifted emission compared to that in absence of Ni. Since no emission band from the TRPL results seems to be related to this transition, it suggests that excitons trapped in these levels tend toward non-radiative recombinations.

Comparing now PL and TRPL results after 1000 °C anneals (Figs. 1 and 3(b)), it is seen that the PL intensity remains relatively high for Ni concentrations between 0.04 and 0.24 at.%., while $\tau_{1/e}$ starts to decrease for Ni concentrations above 0.065 at.%. This means that while the Ni incorporation favours the creation of NRRC, its role in the a-Si crystallisation still contributes more importantly to the PL emission. In order to understand the interplay between these two effects, we have developed a simple model to describe the PL intensity behaviour as a function of Ni concentration. PL intensity is proportional to the number of radiative Si-nc ($N_{\text{Si-nc}}$) and inversely proportional to the radiative decay time τ_{rad}:

$$I \propto \frac{N_{\text{Si-nc}}}{\tau_{\text{rad}}}. \tag{1}$$

In a first approximation, we consider a system where Si-nc and Ni concentrations are both uniform. Also, for annealing at 1000 and 1100 °C, we consider that the Si cluster concentration (N_0) does not vary with temperature. It is known that a-Si clusters form precipitates within the first 5 min of an annealing in silica [4]. We consider for simplicity that a-Si clusters are all the same size with a volume V_c and a spherical shape. TEM measurements (not shown) on a sample containing 9 at.% Si_{xs} annealed at 1050 °C for 1 h show clusters with a 3.2 ± 0.3 nm diameter. Since the annealing temperature does not have a significant impact on the average Si-nc size [16], we estimate $V_c = 17\ nm^3$. We then assume that Ni atoms do not diffuse and remain either inside or outside a-Si at the beginning of an annealing when clusters are formed. It could be argued that Ni can diffuse more rapidly in implanted, thus damaged, silica. Given its high reactivity with Si, Ni may concentrate inside the Si clusters. However, Ni could also react with the significant amount of excess Si remaining in solution [17] in implanted silica even after annealing. We retain the hypothesis of locally uniform Ni distribution, which allows us to estimate the probability to find a Ni atom inside a cluster using Poisson's statistics. As we have discussed earlier, the presence of Ni can increase the PL intensity by inducing a-Si crystallisation, but also acts as a NRRC. We suggest, in our model, that the presence of a single Ni atom in a cluster promotes its crystallization while the presence of more than one Ni atom kills the PL. From these hypothesis and Eq. (1), the expression for PL intensity is:

$$I \propto \frac{N_0 p(e^{-N_{\text{Ni}}V_c} + N_{\text{Ni}}V_c e^{-N_{\text{Ni}}V_c}) + N_0(1-p)(N_{\text{Ni}}V_c e^{-N_{\text{Ni}}V_c})}{\tau_{\text{rad}}}, \tag{2}$$

where p is the fraction of Si clusters already crystallised without Ni, and N_{Ni} is the Ni concentration. The left term in the numerator corresponds to the population for clusters that have been crystallised and are luminescent in absence of Ni. It takes into account the Si-nc population that contains none or one Ni atom. The right term corresponds to the population of Si clusters that is not luminescent in absence of Ni (because they are amorphous or contain defects) but for which the crystallisation induced by one Ni atom makes them luminescent. The resulting expression is plotted as lines in Fig. 2. We included a small constant to take into account the background noise during the PL measurements and we considered N_0/τ_{rad} as a constant factor. For 1000 °C annealing, we assumed a fraction $p = 7\%$ in order for the model to reach the measured PL intensity of the samples containing no Ni. This value is consistent with the low crystallisation rate of Si clusters at such temperature in the absence of Ni.

Considering all these approximations, the qualitative agreement with experimental results, especially for the peak near 0.1 at.% Ni, is satisfactory. This indicates that the model grasps most of the effect of Ni by assuming that the presence of one Ni atom within an a-Si cluster is beneficial while more than one is detrimental. For 1100 °C annealing, we considered $p = 100\%$ so that the PL intensity decreases with the Ni concentration, as do the experimental data. The model, however, underestimates the initial increase in experimental PL intensity. This deviation may originate from the choice of τ_{rad} which could change with the Ni concentration. Still, for both annealing temperatures, the PL intensity predicted by the model and shown by the experimental data disappears for Ni concentration higher then 1 at.%. At this concentration, each Si-nc contains an average of 3–4 Ni atoms, which is consistent with the hypothesis that only Si-nc containing none or one Ni atom are luminescent.

4. Conclusion

In this study, we found that for samples annealed at 1000 °C, Ni incorporation can improve the Si-nc luminescence by up to a factor of 5 with 0.15 at.% Ni. However, this emission remains smaller than for samples annealed at 1100 °C. Higher concentrations of Ni eventually completely kill the PL; this happens around 1 at.% Ni. We

also report two emission bands around 730 and 880 nm, respectively, that have different $\tau_{1/e}$ evolutions with the Ni concentration. If the emission band at 730 nm is related to excited oxygen-passivated surface state, it suggests that Ni modifies the Si-nc/SiO_2 interface. For the band around 880 nm, we suggest that it is related to the fact that the co-implanted Ni promotes a-Si crystallisation. The proposed model indicates that while one Ni atom in a cluster is beneficial by promoting cluster crystallisation and defects annealing, more than one leads to NRRC creation that are responsible for the decreasing emission with increasing Ni content.

Acknowledgements

The authors would like to thank Louis Godbout, Ghaouti Bentoumi and Richard Leonelli for their assistance. This work was supported by the Natural Sciences and Engineering Research Council of Canada, the Fonds québécois de la recherche sur la nature et les technologies, NanoQuébec and Plasmionique Inc.

References

[1] L.T. Canham, Appl. Phys. Lett. 57 (1990) 1046.
[2] X.D. Pi, O.H.Y. Zalloum, T. Roschuk, J. Wojcik, A.P. Knights, P. Masher, P.J. Simpson, Appl. Phys. Lett. 88 (2006) 103111.
[3] D. Barba, F. Martin, G.G. Ross, Nanotechnology 19 (2008) 115707.
[4] Y.Q. Wang, R. Smirani, G.G. Ross, J. Cryst. Growth 294 (2006) 486.
[5] B. Mohadjeri, J. Linnros, B.G. Svensson, M. Östling, Phys. Rev. Lett. 68 (1992) 1872.
[6] Y. He, K. Ma, L. Bi, J.Y. Feng, Z.J. Zhang, Appl. Phys. Lett. 88 (2006) 031905.
[7] L. Bi, Y. He, J.Y. Feng, Z.J. Zhang, Nanotechnology 17 (2006) 2289.
[8] M. Cook, C.T. White, Phys. Rev. 59 (1987) 15.
[9] K. Sato, K. Hirakuri, J. Appl. Phys. 97 (2005) 104326.
[10] M. Luppi, S. Ossini, Phys. Rev. B71 (2005) 035340.
[11] G.G. Ross, D. Barba, F. Martin, Int. J. Nanotechnol. 5 (2008) 984.
[12] S. Takeoka, M. Fujii, S. Hayashi, Phys. Rev. B62 (2000) 16820.
[13] Y. Kanemitsu, T. Ogawa, K. Shiraishi, K. Takeda, Phys. Rev. B48 (1993) 7.
[14] H. Lemke, Phys. Status Solidi A99 (1987) 205.
[15] M. Shiraishi, J.U. Sachse, H. Lemke, J. Weber, Mater. Sci. Eng. B58 (1999) 130.
[16] F. Iacona, G. Franzo, C. Spinella, J. Appl. Phys. 87 (2000) 1295.
[17] A. Irrera, F. Iacona, G. Franzo, S. Boninelli, D. Pacifici, M. Miritello, C. Spinella, D. Sanfilippo, G. Di Stefano, P.G. Fallica, F. Priolo, Opt. Mater. 27 (2005) 1031.